

B. Alouache, M. Helaimi, A.B. Djilali, H.A. Gabbar, H. Allouache, A. Yahdou

Optimal tuning of multi-stage PID controller for dynamic frequency control of microgrid system under climate change scenarios

Introduction. In recent years, the use of renewable energy has become essential to preserve the climate from pollution and global warming. To utilize renewable energy more effectively, the microgrid system has emerged, which is a combination of renewable energies such as wind and solar power. However, due to sudden and random climate fluctuations, energy deviation and instability problems have arisen. To address this, storage systems and diesel engines have been incorporated. Nevertheless, this approach has led to another issue: frequency deviation in the microgrid system. Therefore, most recent studies have focused on finding ways to reduce frequency deviation. The **goal** of this work is to study and compare various improvement methods in terms of frequency deviation. **Methodology.** We first simulated the microgrid system using the PID controller based on the following algorithms: krill herd algorithm (KHA) and cuckoo search algorithm (CSA). In the second phase, we replaced the PID controller with the multi-stage PID controller and optimized its parameters using the KHA and the CSA. In the final phase, we tested the response of the microgrid system to these methods under a range of influencing factors. **Results.** The results initially showed the superiority of the KHA over the other algorithms in improving the parameters of the PID controller. In the second phase, the results showed a significant advantage of the multi-stage PID controller in terms of speed and stabilization time, as well as in reducing the frequency deviation compared to the PID controller. **Practical value.** Based on the tests conducted on the microgrid system, we can conclude that the multi-stage PID controller based on the KHA can be relied upon to solve these types of problems within the microgrid system. References 36, tables 4, figures 10.

Key words: microgrid, multi-stage PID controller, frequency control, renewable energy sources, krill herd algorithm, cuckoo search algorithm.

Вступ. В останні роки використання відновлюваної енергії стало необхідним для збереження клімату від забруднення та глобального потепління. Для більш ефективного використання відновлюваної енергії з'явилася система мікромереж, яка є комбінацією відновлюваних джерел енергії, таких як енергія вітру та сонця. Однак через раптові та випадкові коливання клімату виникли проблеми відхилення та нестабільності енергії. Для вирішення цієї проблеми були включені системи зберігання та дизельні двигуни. Проте цей підхід призвів до іншої проблеми: відхилення частоти в системі мікромереж. Тому більшість останніх досліджень було зосереджено на пошуку способів зменшення відхилення частоти. **Метою** роботи є вивчення і порівняння різних методів поліпшення з погляду відхилення частоти. **Методологія.** Спочатку ми змоделювали систему мікромереж з використанням ПІД-регулятора на основі наступних алгоритмів: алгоритм стада криля (КНА) та алгоритм пошуку зозулі (CSA). На другому етапі ми замінили ПІД-регулятор багатоступінчастим ПІД-регулятором та оптимізували його параметри з використанням КНА та CSA. На заключному етапі ми протестували реакцію мікромережевої системи на ці методи при низці факторів, що впливають. **Результати** спочатку показали перевагу КНА над іншими алгоритмами поліпшення параметрів ПІД-регулятора. На другому етапі результати показали значну перевагу багатоступеневого ПІД-регулятора з точки зору швидкості та часу стабілізації, а також зниження відхилення частоти в порівнянні з ПІД-регулятором. **Практична цінність.** На підставі випробувань, проведених на мікромережевій системі, ми можемо зробити висновок, що багатоступеневий ПІД-регулятор на основі КНА може бути використаний для вирішення цих типів проблем мікромережевої системи. Бібл. 36, табл. 4, рис. 10.

Ключові слова: мікромережа, багатоступеневий ПІД-регулятор, частотне керування, відновлювані джерела енергії, алгоритм стада крилів, алгоритм пошуку зозулі.

Introduction. In recent decades, the world has observed an increase in the concentration of CO₂ in the atmosphere, which can be attributed to the heavy reliance on fossil fuels and their derivatives to meet energy needs. This pollution has a number of adverse effects, including detrimental impacts on human health and the climate. These include rising temperatures and an increase in the frequency of natural disasters [1]. Consequently, it has become imperative to identify sustainable solutions to eliminate traditional sources of pollution. One potential solution is to rely on renewable energy sources, such as wind and solar power. These sources are regarded as environmentally benign, pollution-free, widely accessible, and sustainable. Following the technological advancements in renewable energy sources, a novel concept has emerged: the microgrid. This is an innovative solution that integrates various renewable energy sources, in addition to storage systems. A microgrid is a small electrical system that can operate independently or in parallel with the main power grid. It can be argued that microgrid represent a significant advancement in the pursuit of sustainable and clean energy [2].

The primary challenge confronting the microgrid is the maintenance of frequency and energy stability, given

the unpredictable random fluctuations in energy production from renewable sources. These results in an imbalance between the energy demand and the total energy produced. Consequently, storage systems for the microgrid, such as plug-in hybrid electric vehicle (PHEV), have become indispensable due to their efficacy in buffering and their capacity for rapid charging and efficient energy storage [3]. They function as reservoirs for storing energy and as energy suppliers in the event of a deficit in renewable energy sources to power the load. Nevertheless, this approach is not always secure or sustainable for supplying energy to the load [2], which is why a diesel generator (DEG) is added. Although it is a pollutant, it is considered the last resort when solar, wind energy, and storage batteries fail to supply the load with energy [3].

The proposed microgrid system in this study is comprised of a set of photovoltaic (PV) solar cells, wind turbine generators (WTG), and storage systems represented by PHEV [3]. The batteries are charged when there is a surplus of energy from renewable sources and are used to supply energy when there is a deficit from renewable sources to meet the load demand. Furthermore, DEG has been included to provide energy in the event that all

© B. Alouache, M. Helaimi, A.B. Djilali, H.A. Gabbar, H. Allouache, A. Yahdou

renewable energy sources fail to meet the load demand. This solution ensures that the microgrid used in this study can provide energy in all operating conditions [4, 5].

Once the energy supply for loads had been secured, a further issue emerged in the form of frequency deviation, which was caused by random climate fluctuations. Consequently, the majority of researchers have recently focused their attention on the development of control strategies for microgrid systems, employing a variety of controllers and adjusting their parameters through the use of different optimization algorithms. The PID controller has been employed in the majority of industrial applications, primarily due to its simplicity, reasonable cost, and desirable performance. PID controller based on the genetic algorithm has been studied for frequency deviation control in [6, 7] proposed optimizing the parameters of the PID controller using the grey wolf optimization. In [8] proposed optimizing the parameters of the PID controller based on the harmony search algorithm. In [9], frequency control in the microgrid was achieved using the PID controller based on the fruit fly algorithm. In [10] was proposed to control the frequency in the microgrid system using PID based on the algorithm particle swarm optimization (PSO). All the aforementioned research used the PID controller. However, this choice has inherent limitations and is not suitable for these parameters. It may lead to solutions where the values of the optimizers or the controller parameters are minimal. Consequently, the methodology has been revised to incorporate the fractional order PID (FOPID) controller as an alternative to the PID controller. This work was addressed in [11], where he controlled the frequency of the AC microgrid system using the FOPID controller based on a set of optimization algorithms. In [12] was optimized the parameters of the FOPID controller based on the PSO algorithm with the objective of controlling frequency deviation oscillations as well as power. Nevertheless, when examining this type of controller, it became evident that there were still some limitations in applying optimization algorithms to adjust the parameters of the PID controller [10]. Consequently, another controller was employed by other researchers, namely the multi-stage PID (MPID) controller, comprising two distinct controllers, namely PD and PI. In [13] was applied fuzzy logic to determine the parameters of the MPID controller for frequency control of the microgrid. Despite the fact that the fuzzy logic method is considered classical compared to modern optimization algorithms, this study yielded good results. In [14] was used the MPID controller to control the frequency of the isolated microgrid using a set of optimization algorithms. This research resulted in a prompt and effective response to frequency stability issues. In addition, in [15] was investigated frequency and power stability using the MPID controller based on the smell agent optimization. Following the aforementioned studies, the researchers proposed the use of the MPID controller in this study.

MPID is a controller comprising two distinct controllers connected in series. The initial PI controller is tasked with ensuring rapid response and the minimization of undesired distortions. Subsequently, the second PID controller is responsible for maintaining accuracy and

reducing the error rate. This type of controller is highly flexible and capable of handling complex systems such as microgrid. In order to achieve an optimal design of the MPID controller, it is necessary to utilize optimization algorithms in order to determine the optimal values of its parameters [16].

In order to achieve enhanced and more desirable stability in the microgrid system, it is essential to determine the optimal values of the MPID controller constants. In order to achieve this objective, two optimization algorithms were subjected to investigation: the krill herd algorithm (KHA) and the cuckoo search algorithm (CSA) were considered. These are distinct algorithms that belong to the category of nature-inspired or evolutionary algorithms. The fundamental principles of these algorithms have been elucidated in [17–23]. KHA is slower in finding solutions due to its complex calculations related to krill movement. Nevertheless, it is regarded as more efficacious in addressing intricate systems and attaining optimal solutions in comparison to the CSA [17, 18]. Conversely, the CSA is relatively straightforward to implement due to its simplicity in application and design, and it requires minimal information to search the solution space [15, 21–23]. In order to enhance the frequency deviation in the microgrid, a study was conducted to assess the efficacy of these two algorithms when employed with the MPID controller. Consequently, a series of simulations were conducted in MATLAB with the objective of comparing the two algorithms and achieving a stable system. A series of scenarios representing potential operating conditions of the microgrid were conducted. The scenarios included:

- 1) Scenario I. Evaluation of technical response KHA-PID compared to PSO-PID and CSA-PID against disturbance load ΔP_L .
- 2) Scenario II. Evaluating the response of the MPID controller and comparing it with the PID controller using the KHA and CSA against disturbance load ΔP_L .
- 3) Scenario III. In this scenario we compared the two approaches proposed in this research MPID-KHA and MPID-CSA under different possible operating conditions ΔP_L , ΔP_{PV} , ΔP_{WTG} in the microgrid.
- 4) Scenario IV. In this scenario we pointed out the role and effectiveness of electric car batteries in improving and controlling frequency deviation in microgrid.

Microgrid concept. Figure 1 shows a microgrid used in remote electric vehicle charging stations, consisting of two renewable energy sources: solar energy and wind energy.

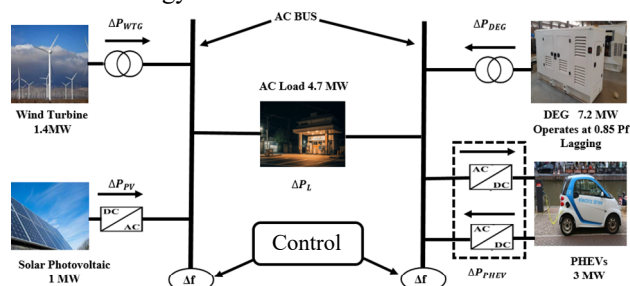


Fig. 1. Structure overview on proposed isolated microgrid system Bella Coola

Due to the random fluctuations in climate that affect energy production and stability [15], storage systems and a

DEG have been incorporated into the system to ensure stability. However, these additions are not sufficient to regulate the frequency deviation of the microgrid. Therefore, the implementation of control systems such as the PID controller and the MPID controller is essential [24].

Modeling of different generation components.

In order to analyze small signals in order to verify the reliability and stability of frequency deviation for the microgrid system, models can be designed. These models can include PV, WTG, DEG and PHEV, which can be modeled by the first-order transfer function. First, starting from Fig. 1, the energy balance equation for the energy released by the microgrid can be written as [14, 15]:

$$P_S = P_{PV} + P_{WTG} + P_{DEG} - P_{PHEV}, \quad (1)$$

where P_S is the total average power generation.

The generation-load balance equation is:

$$\Delta P_L = \Delta P_{PV} + \Delta P_{WTG} + \Delta P_{DEG} - \Delta P_{PHEV}. \quad (2)$$

From (2) we infer that variations in power generation have a significant impact on frequency deviation in the system. Therefore, frequency deviation Δf can be expressed from [25, 26]:

$$TF_S = \frac{\Delta f}{\Delta P_L} = \frac{1}{k_S(1+S \cdot T_S)} = \frac{1}{M \cdot S + D}, \quad (3)$$

where M , D are the equivalent inertia constant and damping constant, respectively; Δf is the frequency deviation; k_S is the gain constant of the microgrid; T_S is the time constant; TF_S is the transfer function of the microgrid; S is the Laplace variable.

From (3), (4) the frequency deviation of the microgrid system can be expressed as:

$$\Delta f = \frac{1}{M \cdot S + D} [\Delta P_{PV} + \Delta P_{WTG} + \Delta P_{DEG} - \Delta P_{PHEV}]. \quad (4)$$

In order to study the variations in frequency deviation, it is necessary to examine each element of the energy sources connected to the microgrid.

Model of PV generation system. Solar energy is cheap and easy to make and install. It is made up of a set of connected PV cells, either in parallel or series. These cells turn sunlight into electricity. This can be expressed as [24–27]:

$$TF_{PV} = \frac{\Delta P_{PV}}{\Delta \phi} = \frac{K_{PV}}{1+S \cdot T_{PV}}, \quad (5)$$

where TF_{PV} is the transfer function of the PV system; ΔP_{PV} is the change in output power; $\Delta \phi$ is the change in solar irradiance; K_{PV} is the gain constant of the PV; T_{PV} is the time constant.

Model of the wind energy. Wind energy involves converting kinetic energy into electrical energy through the rotation of large turbines directly connected to the rotor of the electrical generator. It can be expressed mathematically as [25–27]:

$$TF_{WTG} = \frac{K_{WTG}}{1+S \cdot T_{WTG}}, \quad (6)$$

where TF_{WTG} is the transfer function; K_{WTG} is the gain constant of the WTG; T_{WTG} is the time constant.

DEG model. DEG is a traditional source of power production and is used in cases of renewable energy system failure and energy storage systems to supply power to the load. It represents a reliable source for providing energy to the microgrid and can be expressed as [24, 25]:

$$TF_{DEG} = \frac{K_{DEG}}{1+S \cdot T_{DEG}}, \quad (7)$$

where TF_{DEG} is the transfer function of the DEG; K_{DEG} is the gain constant of the DEG; T_{DEG} is the time constant.

PHEV model. Electric vehicles are considered an important element in this work as they serve two functions: acting as a load and serving as a source for energy storage and load financing in case renewable energy sources fail. They represent an alternative for energy storage to meet needs in controlling frequency deviations in the microgrid. The energy present in electric vehicles can be expressed based on frequency deviation as [28]:

$$\Delta P_{PHEV} = \begin{cases} -\Delta P_{\max} \cdot U_C < -\Delta P_{\max}; \\ -\Delta P_{\max} \cdot U_C > -\Delta P_{\max}; \\ U_C \cdot |U_C| \leq \Delta P_{\max}. \end{cases} \quad (8)$$

where U_C is the output signal determines whether the ΔP_{PHEV} will be employed for either charging or discharging purposes [28]; P_{\max} is the maximum power that can be obtained from an individual electric vehicle.

The battery's state of charge (SOC) influences the value of K_{EV} (Fig. 2) depicting the relationship between K_{EV} and SOC for PHEV [29, 30].

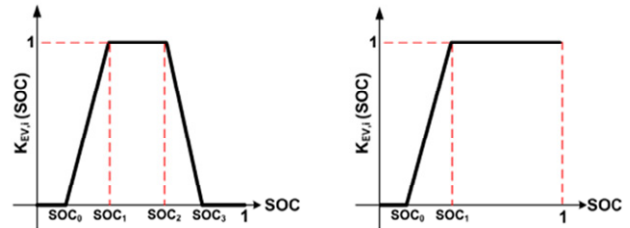


Fig. 2. Representing the charging and discharging PHEV

Following analysis and simplification, the ultimate mathematical expression can be represented in the format of a first-order simplifier:

$$\Delta P_{PHEV} = \frac{N_{EV} \left[\Delta U_C - \Delta f \cdot \frac{K_{EV}}{R_{av}} \right]}{1+S \cdot T_{EV}}, \quad (9)$$

where ΔP_{PHEV} is the energy generated by a single PHEV; N_{EV} is the total number of electric vehicles; ΔU_C is the controller's output signal; Δf is the frequency deviation; K_{EV} is the gain constant of the PHEV; R_{av} is the droop characteristics of the PHEV; T_{EV} is the battery time constant [28].

MPID controller and objective function. MPID controller is a controller that has the same general concept as a classical controller PID controller in that it adjusts or corrects deviations between the measured variable and the desired set point [16]. It consists of two units PD and PI connected in series (Fig. 3).

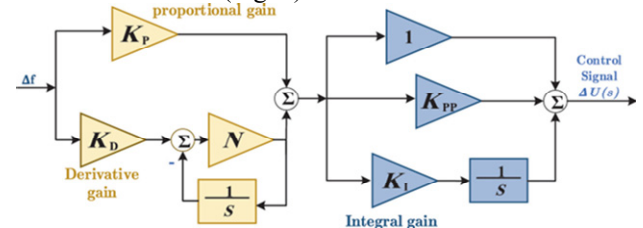


Fig. 3. Block diagram of MPID controller

The unit PD is the first one, and its input is the distortion ratio at the frequency Δf and its output is the

input to unit PI. The output of unit PI serves as an enhanced signal for the frequency using ΔU_c . One of the advantages of unit MPID is that all controller parameters in all stages of frequency variation for the microgrid system can be maximally utilized [13].

MPID controller has an advantage over the classic controller, as it can use the best features of both controllers PD and PI controllers. In the PI controller, the integral term must exist during steady state and the output is constant to the PD controller. This means that the integrated output will be zero during the transient, avoiding the limitation of classical PID. This controller has been successfully applied to many engineering problems [13]. MPID controller is connected to the microgrid and can be implemented as shown in Fig. 4. The mathematical model of the MPID controller can be expressed as:

$$\frac{\Delta U_c}{\Delta f} = (K_p + K_d \cdot S) \cdot \left(1 + K_{pp} + \frac{K_i}{S}\right), \quad (10)$$

where ΔU_c is the control signal; K_i is the integral gain; K_p is the proportional gain; K_d is the derivative gain; K_{pp} is the additional proportional gain.

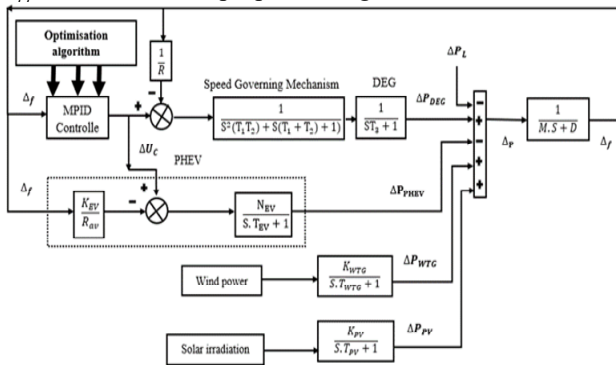


Fig. 4. Dynamic model of the proposed isolated microgrid

Table 1 represents list of all microgrid constants.

Table 1

List of all microgrid constants

Parameter	Value	Parameter	Value
$M(S)$	0.1667	T_1	0.025
$D(MW)$	0.015	T_2	2
$T_{PI}(S)$	1.8	T_3	3
T_{WTG}	2	K_{PV}	1
T_{EV}	0.1	K_{WTG}	1
$R_{av}(Hz/MW)$	2.4	N_{EV}	600

Objective function and optimization of MPID controller. The disturbances that cause deviations in the frequency of the microgrid system are a result of random fluctuations in the production of energy, especially from renewable energy sources [19]. Addressing this issue requires precise and quick adjustments in the controller parameters. To tackle this problem, we have studied the following two algorithms:

Overview of KHA. KHA is an optimization algorithm inspired by the natural behavior of a krill swarm, where it relies on collective behavior in searching for nesting areas, food and encounter and move away from predators. The main components of the KHA include [31–33]: krill individuals; krill swarm leader; interaction among swarm individuals; selection and adaptation.

In the KHA each solution can be represented by the foraging space or the distance between it and the

predators, and the solutions can be expressed in the following mathematical form [32]:

• To determine the optimal location for food abundance we use the following relationship:

$$\Delta x_i^a = a \sum_{j=1}^N \frac{f(x_j) - f(x_i)}{\|x_j - x_i\|}. \quad (11)$$

• To determine the distance of a hard krill herd from enemies, we use the following mathematical relationship:

$$\Delta x_i^r = B \sum_{j=1}^N \frac{1}{\|x_j - x_i\|}. \quad (12)$$

• Finally, to determine the safe space for swarm stability, which is the ideal and best solution, we use the following mathematical relationship:

$$x_j(t+1) = x_j(t) + \Delta x_i^a + \Delta x_i^r, \quad (13)$$

where Δx^a is the new value of dining space; Δx^r is the new value for the swarm's distance from the enemy; x_j is the new candidate solution that replaces the less-fit solution x_i is the current solution within the search space; N is the number of solutions; a, B are the interaction coefficients for attraction and repulsion; $f(x_j)$ and $f(x_i)$ are the objective function values for solutions j and i , respectively.

Application of KHA to optimize the MPID controller. At this stage we explain how to improve the MPID controller using the algorithm:

Step 1 – initialization. Choose random search spaces using (12) and (13). Since the proposed controller contains (K_p, K_d, K_{pp}, K_i) as 4 basic control parameters, start by searching for random solutions of the parameters.

Step 2 – evaluate solutions. At this stage we evaluate the solutions using (15).

Step 3 – selection. We mark the best solution and update the parameters MPID controller of the KHA.

Step 4 – algorithm termination. At the end of the iterations number, the algorithm chooses the best solution.

Cuckoo search algorithm. CSA was proposed in [17], inspired by the natural life of the cuckoo bird. The strategy relies on the reproductive behavior of the female cuckoo, which lays its eggs in the nests of other bird species to avoid the effort of building nests and caring for the eggs and chicks. This algorithm focuses on two main conditions for its success [34–36]:

• the female cuckoo randomly selects the best nests built by other birds;

• the female cuckoo disposes of the eggs far away from the nest and lays her own eggs at each stage. She repeats this process until only one egg from the other species remains.

Eggs are the primary problem in this algorithm, with the cuckoo's egg being the new solution generated. This solution is calculated using the Levy Flight distribution as follows [33]:

$$x_j(t+1) = x_i(t) + a \cdot \text{levy}(\lambda); \quad (14)$$

$$\text{levy}(\lambda) = s \cdot (x_i(t) - x_{best}); \quad (15)$$

where x_j is the new candidate solution that replaces the less-fit solution; x_i is the current solution in the search space; λ is the Levy exponent; a is the constant; x_{best} is the best current solution; $i = 1, 2, 3, \dots, N$:

$$s = \sigma_u \cdot |u|^{-1/\beta}. \quad (16)$$

where s is the step size used to update solutions in the algorithm, σ_u is the scaling factor or coefficient that determines the overall impact of the step size; u is a random variable generated from a Levy distribution; V is the distance between the current solution and the best existing solution; β is the parameter that controls the behavior of the power-law of the system

If the host bird detects the cuckoo egg, it means that the condition $x_j < x_i$ is true, the host bird discards this cuckoo egg (the new solution is modified) and it is replaced with a new solution calculated as follows:

$$x_j(t+1) = x_i(t) + \text{rand}(n_1 - n_2) \text{ for } n_1, n_2, \dots, N. \quad (17)$$

Application of CSA algorithm to optimize the MPID controller.

Step 1 – initialization. Proposing a number of random solutions within the nest search area, we then evaluate each solution using the objective function.

Step 2 – MPID controller initialization. Initialize K_p, K_i, K_d, K_{pp} parameters and error conditions (current error, cumulative error, and previous error).

Step 3. At each iteration, we adjust the MPID controller parameters using Levy trips.

Step 4. Repeat the above steps until convergence or the maximum number of iterations is reached.

Step 5 – best solution. We select the best set of parameters found during the search for the MPID controller.

Begin

Define the objective function

Define the maximum number (n) of iterations and other parameters

while ($x < \text{MaxGeneration}$):

Obtain a cuckoo randomly via Levi's flights and then we determine the MPID parameters

Evaluate its fitness F_i

Choose a nest among n (say j) randomly

if $x_i > x_j$

Replace F_j with the new parameters

End if

End while

A group of bad nests is abandoned, and one nest is chosen as the best solution, which expresses the values of the constants for MPID controller.

End.

Results and discussions. We evaluated the performance of the isolated microgrid system using a MATLAB/Simulink in a time domain of 250 s (Fig. 2). We applied KHA and CSA to improve the parameters of MPID controller for good control of the frequency deviation of the system. In addition to comparing them, we conducted a set of operating scenarios for the microgrid, which are as follows.

Scenario I. Evaluation of technical response KHA-PID compared to PSO-PID and CSA-PID against disturbance load ΔP_L . In this scenario, we simulated the microgrid using the PID controller optimized with KHA, CSA and PSO. As Table 2 shows the values for PID controller optimized with these algorithms, we also compared these results in Fig. 5 showed the superiority of the KHA in terms of speed in stability time, as well as a decrease in unwanted frequency changes. Then followed by

the CSA, which also showed its superiority over PSO algorithm. Given these results obtained, they are considered undesirable. Therefore, it has become necessary to search for another approach and work on it.

Table 2

Optimal parameters of the PID controller based on PSO, KHA and CSA

Methods	Optimized gains			
	K_p	K_i	K_d	N
PSO-PID	1.032	1.624	1.1992	100.226
CSA-PID	1.395	1.4281	1.9078	59.26
KHA-PID	2.4702	2.670	1.01	78.3

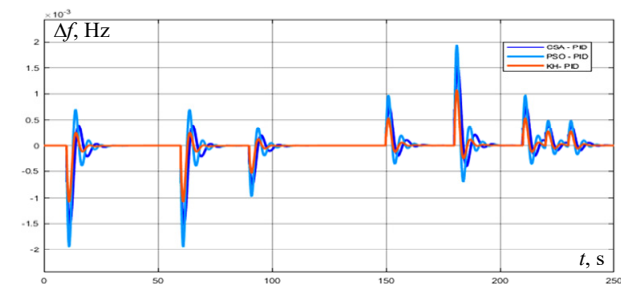


Fig. 5. Frequency disturbance response in the microgrid system using PSO-PID, CSA-PID, KHA-PID

Scenario II. Evaluating the response of the MPID controller and comparing it with the PID controller using the KHA and CSA against disturbance load ΔP_L .

In this scenario, we performed frequency deviation simulations using PID and MPID controllers with an optimization algorithm. Table 3 shows the numerical values for each parameter of these controllers. The results (Fig. 6) showed the extent of the superiority of the MPID controller in reducing unwanted frequency deviations compared to PID controller despite using 2 different types of optimization algorithms.

Table 3

Optimal parameters of the MPID controllers based KHA and CSA

Methods	Optimized gains				
	K_p	K_i	K_d	K_{pp}	N
KHA-MPID	4.9736	4.3943	4.5787	0.490	36.753
CSA-MPID	4.650	2.05	2.980	0.297	28.962

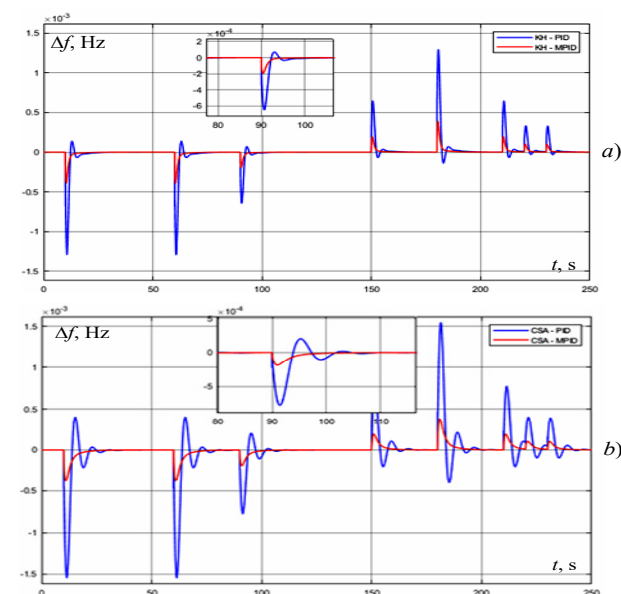


Fig. 6. Microgrid frequency disturbance response using KHA-PID (a) and CSA-PID (b)

Scenario III. In this scenario, we compared the two approaches proposed in this research MPID-KHA and MPID-CSA under different possible operating conditions (ΔP_L , ΔP_{pv} , ΔP_{WTG}) in the microgrid. In this scenario, we tested frequency drift under a different set of influences and obstacles to the microgrid, namely stochastic changes in climate. We implemented a number of simulation cases as follows.

Case 1. In this case, we place the microgrid under ΔP_L , which represents the energy change in the batteries (Fig. 7,a). Figure 7,b represents the frequency deviation response Δf in the microgrid.

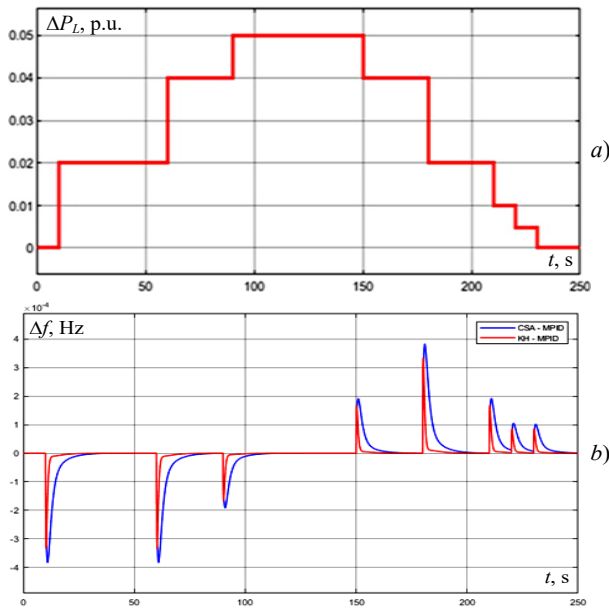


Fig. 7. Frequency disturbance response of KHA-MPID and CSA-MPID under load disturbances ΔP_L

Case 2. In this case, we disconnected the battery source and the solar energy source, and connected only the wind energy ΔP_{WTG} (Fig. 8,a). Figure 8,b represents the frequency deviation Δf in this case.

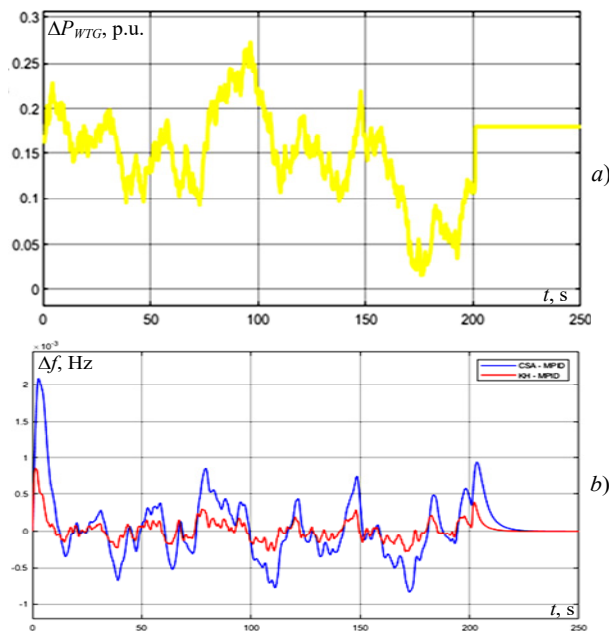


Fig. 8. Frequency disturbance response of KHA-MPID and CSA-MPID under wind energy ΔP_{WTG}

Case 3. In this case, we also disconnected the battery source as well as the wind power source, and connected only the solar power ΔP_{pv} (Fig. 9,a). Figure 9,b represents the frequency deviation Δf in this case.

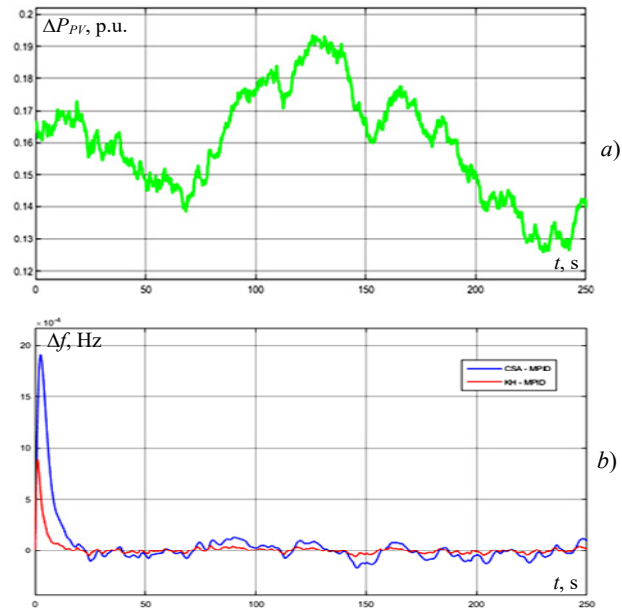


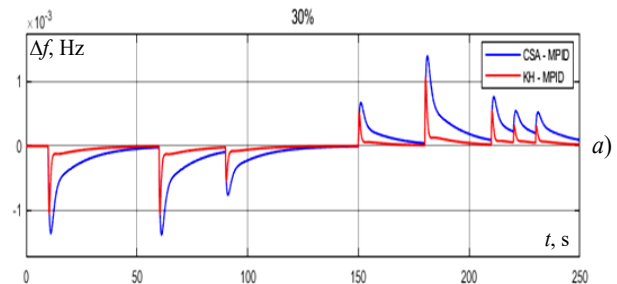
Fig. 9. Frequency disturbance response of KHA-MPID and CSA-MPID under ΔP_{pv}

The objective of these 3 cases is to demonstrate the superiority of the proposed approaches in controlling frequency deviation under various factors affecting the microgrid. Through these results, we observe the significant superiority of KHA-MPID over CSA-MPID in terms of greatly reducing the frequency distortion percentage as well as the speed in reaching the stability state or the settling time.

Scenario IV. In this scenario, we pointed out the role and effectiveness of PHEV in improving and controlling frequency deviation in microgrid. Table 4 represents the percentage of change in electric car batteries (charge rate) as we connect the batteries to the microgrid system. The results in Fig. 10 show that batteries play a major role in reducing and improving frequency deviation, and therefore we say that the storage system has great effectiveness in improving the performance of the microgrid system.

Table 4

Percentage variation, %	Parameters PHEVs			
	R_{pv}	T_{EV}	K_{EV}	N_{EV}
±30	0.72	0.03	0.54	180
±50	1.2	0.05	0.9	300
±70	1.68	0.07	1.26	420



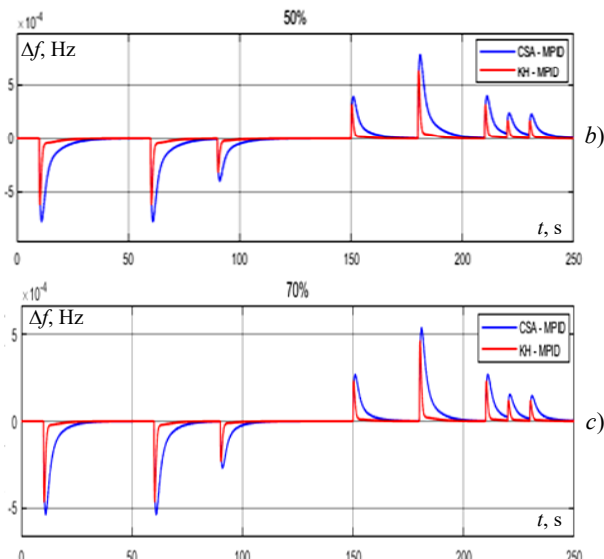


Fig. 10. Effect of frequency deviation in the microgrid versus a difference in battery charge percentage of $\pm 30\%$ (a); $\pm 50\%$ (b); $\pm 70\%$ (c)

Conclusions. In this research we proposed a study to propose an approach to control the frequency deviation of the microgrid system caused by random climate changes. Therefore, we used the MPID controller with two optimization algorithms (KHA and CSA) to adjust the parameters of the controller.

To verify the effectiveness of this approach, we initially compared it with the PID controller based on the same two algorithms. The obtained results demonstrated the superiority of the proposed approach in terms of system stability in terms of faster settling time and lower distortion ratio in the deviation. In the second phase, we confirmed the robustness of this approach in controlling the frequency deviation by conducting several potential impact scenarios. We also demonstrated the superiority of the KHA over CSA using the MPID controller. Finally, based on previous studies and the results obtained in this study, we can confirm that the MPID controller based on the KHA can be relied upon to solve these types of problems, such as controlling frequency deviation in a microgrid.

Conflict of interest. The authors of the article declare that there is no conflict of interest.

REFERENCES

1. Leroutier M., Quirion P. Air pollution and CO2 from daily mobility: Who emits and Why? Evidence from Paris. *Energy Economics*, 2022, vol. 109, art. no. 105941. doi: <https://doi.org/10.1016/j.eneco.2022.105941>.
2. Alhamrouni I., Wahab W., Salem M., Rahman N.H.A., Awal L. Modeling of micro-grid with the consideration of total harmonic distortion analysis. *Indonesian Journal of Electrical Engineering and Computer Science*, 2019, vol. 15, no. 2, pp. 581-592. doi: <https://doi.org/10.11591/ijeecs.v15.i2.pp581-592>.
3. Sathish C., Chidambaram I.A., Manikandan M. Intelligent cascaded adaptive neuro fuzzy interface system controller fed KY converter for hybrid energy based microgrid applications. *Electrical Engineering & Electromechanics*, 2023, no. 1, pp. 63-70. doi: <https://doi.org/10.20998/2074-272X.2023.1.09>.
4. Manikandan K., Sasikumar S., Arulraj R. A novelty approach to solve an economic dispatch problem for a renewable integrated micro-grid using optimization techniques. *Electrical Engineering & Electromechanics*, 2023, no. 4, pp. 83-89. doi: <https://doi.org/10.20998/2074-272X.2023.4.12>.
5. Belbachir N., Zellaoui M., Settoul S., El-Bayeh C.Z., Bekkouche B. Simultaneous optimal integration of photovoltaic distributed generation

- and battery energy storage system in active distribution network using chaotic grey wolf optimization. *Electrical Engineering & Electromechanics*, 2021, no. 3, pp. 52-61. doi: <https://doi.org/10.20998/2074-272X.2021.3.09>.
6. Das D.C., Roy A.K., Sinha N. GA based frequency controller for solar thermal-diesel-wind hybrid energy generation/energy storage system. *International Journal of Electrical Power & Energy Systems*, 2012, vol. 43, no. 1, pp. 262-279. doi: <https://doi.org/10.1016/j.ijepes.2012.05.025>.
7. Srinivasarathnam C., Yammani C., Maheswarapu S. Load Frequency Control of Multi-microgrid System considering Renewable Energy Sources Using Grey Wolf Optimization. *Smart Science*, 2019, vol. 7, no. 3, pp. 198-217. doi: <https://doi.org/10.1080/23080477.2019.1630057>.
8. Shankar R., Kumar A., Raj U., Chatterjee K. Fruit fly algorithm-based automatic generation control of multiarea interconnected power system with FACTS and AC/DC links in deregulated power environment. *International Transactions on Electrical Energy Systems*, 2019, vol. 29, no. 1, art. no. e2690. doi: <https://doi.org/10.1002/etep.2690>.
9. Kalyan C.N.S., Goud B.S., Kumar M.K., Bajaj M., Rubanenko O., Danylenko D. Fruit Fly Optimization Algorithm Tuned 2DOFPID Controller for Frequency Regulation of Dual Area Power System With AC-DC Lines. *2022 IEEE 3rd KhPI Week on Advanced Technology (KhPIWeek)*, 2022, pp. 1-6. doi: <https://doi.org/10.1109/KhPIWeek57572.2022.9916505>.
10. Regad M., Helaimi M., Taleb R., Toubal Maamar A.E. Optimum Synthesis of the PID Controller Parameters for Frequency Control in Microgrid Based Renewable Generations. *Lecture Notes in Networks and Systems*, 2020, vol. 102, pp. 546-556. doi: https://doi.org/10.1007/978-3-030-37207-1_58.
11. Yang C., Yao W., Fang J., Ai X., Chen Z., Wen J., He H. Dynamic event-triggered robust secondary frequency control for islanded AC microgrid. *Applied Energy*, 2019, vol. 242, pp. 821-836. doi: <https://doi.org/10.1016/j.apenergy.2019.03.139>.
12. Regad M., Helaimi M., Taleb R., Othman A.M., Gabbar H.A. Frequency Control in Microgrid Power System with Renewable Power Generation Using PID Controller Based on Particle Swarm Optimization. *Lecture Notes in Networks and Systems*, 2020, vol. 102, pp. 3-13. doi: https://doi.org/10.1007/978-3-030-37207-1_1.
13. Annamraju A., Nandiraju S. A novel fuzzy tuned multistage PID approach for frequency dynamics control in an islanded microgrid. *International Transactions on Electrical Energy Systems*, 2020, vol. 30, no. 12, art. no. e12674. doi: <https://doi.org/10.1002/2050-7038.12674>.
14. Khadanga R.K., Padhy S., Panda S., Kumar A. Design and analysis of multi-stage PID controller for frequency control in an islanded micro-grid using a novel hybrid whale optimization-pattern search algorithm. *International Journal of Numerical Modelling: Electronic Networks, Devices and Fields*, 2018, vol. 31, no. 5, art. no. e2349. doi: <https://doi.org/10.1002/jnm.2349>.
15. Louarem S., Kebbab F.Z., Salhi H., Nouri H. A comparative study of maximum power point tracking techniques for a photovoltaic grid-connected system. *Electrical Engineering & Electromechanics*, 2022, no. 4, pp. 27-33. doi: <https://doi.org/10.20998/2074-272X.2022.4.04>.
16. Sahu P.C., Prusty R.C., Panda S. Optimal design of a robust FO-Multistage controller for the frequency awareness of an islanded AC microgrid under i-SCA algorithm. *International Journal of Ambient Energy*, 2022, vol. 43, no. 1, pp. 2681-2693. doi: <https://doi.org/10.1080/01430750.2020.1758783>.
17. Ali Moussa M., Derrouazin A., Latroch M., Aillerie M. A hybrid renewable energy production system using a smart controller based on fuzzy logic. *Electrical Engineering & Electromechanics*, 2022, no. 3, pp. 46-50. doi: <https://doi.org/10.20998/2074-272X.2022.3.07>.
18. Gandomi A.H., Talatahari S., Tadbiri F., Alavi A.H. Krill herd algorithm for optimum design of truss structures. *International Journal of Bio-Inspired Computation*, 2013, vol. 5, no. 5, art. no. 281-288. doi: <https://doi.org/10.1504/IJBIC.2013.057191>.
19. Yaghoobi S., Mojallali H. Tuning of a PID controller using improved chaotic Krill Herd algorithm. *Optik*, 2016, vol. 127, no. 11, pp. 4803-4807. doi: <https://doi.org/10.1016/j.jileo.2016.01.055>.
20. Bolaji A.L., Al-Betar M.A., Awadallah M.A., Khader A.T., Abualigah L.M. A comprehensive review: Krill Herd algorithm (KH) and its applications. *Applied Soft Computing*, 2016, vol. 49, pp. 437-446. doi: <https://doi.org/10.1016/j.asoc.2016.08.041>.
21. Sarda J., Pandya K., Lee K.Y. Hybrid cross entropy – cuckoo search algorithm for solving optimal power flow with renewable generators and

- controllable loads. *Optimal Control Applications and Methods*, 2023, vol. 44, no. 2, pp. 508-532. doi: <https://doi.org/10.1002/oca.2759>.
22. Barrat J.-L., Del Gado E., Egelhaaf S.U., Mao X., Dijkstra M., Pine D.J., Kumar S.K., (...), Kwon J. Soft matter roadmap. *Journal of Physics: Materials*, 2024, vol. 7, no. 1, art. no. 012501. doi: <https://doi.org/10.1088/2515-7639/ad06cc>.
23. Abdellah A., Larbi M., Toumi D. Open circuit fault diagnosis for a five-level neutral point clamped inverter in a grid-connected photovoltaic system with hybrid energy storage system. *Electrical Engineering & Electromechanics*, 2023, no. 6, pp. 33-40. doi: <https://doi.org/10.20998/2074-272X.2023.6.06>.
24. Ayat Y., Badoud A.E., Mekhilef S., Gassab S. Energy management based on a fuzzy controller of a photovoltaic/fuel cell/Li-ion battery/supercapacitor for unpredictable, fluctuating, high-dynamic three-phase AC load. *Electrical Engineering & Electromechanics*, 2023, no. 3, pp. 66-75. doi: <https://doi.org/10.20998/2074-272X.2023.3.10>.
25. Mohamed R., Helaimi M., Taleb R., Gabbar H.A., Othman A.M. Frequency control of microgrid system based renewable generation using fractional PID controller. *Indonesian Journal of Electrical Engineering and Computer Science*, 2020, vol. 19, no. 2, pp. 745-755. doi: <https://doi.org/10.11591/ijeecs.v19.i2.pp745-755>.
26. Khan S.A., Mahmood T., Awan K.S. A nature based novel maximum power point tracking algorithm for partial shading conditions. *Electrical Engineering & Electromechanics*, 2021, no. 6, pp. 54-63. doi: <https://doi.org/10.20998/2074-272X.2021.6.08>.
27. Kumar R.S., Reddy C.S.R., Chandra B.M. Optimal performance assessment of intelligent controllers used in solar-powered electric vehicle. *Electrical Engineering & Electromechanics*, 2023, no. 2, pp. 20-26. doi: <https://doi.org/10.20998/2074-272X.2023.2.04>.
28. Latif A., Pramanik A., Das D.C., Hussain I., Ranjan S. Plug in hybrid vehicle-wind-diesel autonomous hybrid power system: frequency control using FA and CSA optimized controller. *International Journal of System Assurance Engineering and Management*, 2018, vol. 9, no. 5, pp. 1147-1158. doi: <https://doi.org/10.1007/s13198-018-0721-1>.
29. Zerzouri N., Ben Si Ali N., Benalia N. A maximum power point tracking of a photovoltaic system connected to a three-phase grid using a variable step size perturb and observe algorithm. *Electrical Engineering & Electromechanics*, 2023, no. 5, pp. 37-46. doi: <https://doi.org/10.20998/2074-272X.2023.5.06>.
30. Khemis A., Boutabba T., Drid S. Model reference adaptive system speed estimator based on type-1 and type-2 fuzzy logic sensorless control of electrical vehicle with electrical differential. *Electrical Engineering & Electromechanics*, 2023, no. 4, pp. 19-25. doi: <https://doi.org/10.20998/2074-272X.2023.4.03>.
31. Laifa A., Ayachi B. Application of whale algorithm optimizer for unified power flow controller optimization with consideration of renewable energy sources uncertainty. *Electrical Engineering & Electromechanics*, 2023, no. 2, pp. 69-78. doi: <https://doi.org/10.20998/2074-272X.2023.2.11>.
32. Mahdad B., Srairi K. Interactive artificial ecosystem algorithm for solving power management optimizations. *Electrical Engineering & Electromechanics*, 2022, no. 6, pp. 53-66. doi: <https://doi.org/10.20998/2074-272X.2022.6.09>.
33. Tebbakh N., Labed D., Labed M.A. Optimal size and location of distributed generations in distribution networks using bald eagle search algorithm. *Electrical Engineering & Electromechanics*, 2022, no. 6, pp. 75-80. doi: <https://doi.org/10.20998/2074-272X.2022.6.11>.
34. Mezhoud N., Ayachi B., Amarouyache M. Multi-objective optimal power flow based gray wolf optimization method. *Electrical Engineering & Electromechanics*, 2022, no. 4, pp. 57-62. doi: <https://doi.org/10.20998/2074-272X.2022.4.08>.
35. Vo D.N., Schegner P., Ongsakul W. Cuckoo search algorithm for non-convex economic dispatch. *IET Generation, Transmission & Distribution*, 2013, vol. 7, no. 6, pp. 645-654. doi: <https://doi.org/10.1049/iet-gtd.2012.0142>.
36. Thao N.T.P., Thang N.T. Environmental Economic Load Dispatch with Quadratic Fuel Cost Function Using Cuckoo Search Algorithm. *International Journal of U- and e-Service, Science and Technology*, 2014, vol. 7, no. 2, pp. 199-210. doi: <https://doi.org/10.14257/ijunesst.2014.7.2.19>.

Received 19.06.2024
Accepted 15.08.2024
Published 02.01.2025

B. Alouache¹, PhD Student,
M. Helaimi¹, PhD, Associate Professor,
A.B. Djilali¹, Doctor of Electrical Engineering,
H.A. Gabbar², Full Professor,
H. Allouache¹, Doctor of Electrical Engineering,
A. Yahdou¹, Doctor of Electrical Engineering,
¹Electrical Engineering Department,
Laboratoire Génie Electrique et Energies Renouvelables
(LGEER), Hassiba Benbouali University, Chlef, Algeria,
e-mail: b.alouache@univ-chlef.dz (Corresponding Author);
²Department of Energy and Nuclear Engineering,
Faculty of Engineering and Applied Science,
University of Ontario Institute of Technology (UOIT), Canada.

How to cite this article:

Alouache B., Helaimi M., Djilali A.B., Gabbar H.A., Allouache H., Yahdou A. Optimal tuning of multi-stage PID controller for dynamic frequency control of microgrid system under climate change scenarios. *Electrical Engineering & Electromechanics*, 2025, no. 1, pp. 8-15. doi: <https://doi.org/10.20998/2074-272X.2025.1.02>